vehicles

MDPI

Article

Excitation Parameters Effect on Damper Performance Through Experimental Analysis

Alexandru Dobre *, Gabriel Burduș, Vicentziu-Constantin Mihăilă and Răzvan-Alexandru Durigon

Automotive Engineering Department, National University of Science and Technology POLITEHNICA Bucharest, 060042 Bucharest, Romania; burdusgabriel@gmail.com (G.B.); vicentziumihaila@yahoo.com (V.-C.M.); razvandurigon@protonmail.com (R.-A.D.)

* Correspondence: alexandru.dobre@upb.ro

Abstract

Nowadays, the automotive industry is facing an increasing demand for comfort, handling, and stability; thus, the suspension system plays a crucial role in ensuring these modern requirements. The growing need for improved dampers requires a deeper understanding of how shock absorbers behave under certain conditions. Consequently, experimental analysis of damping systems represents an essential step in the development process of an advanced and modern suspension system. This paper aims to present an experimental investigation of shock absorber behaviour using a dedicated testing stand designed to evaluate the damping phenomenon and how it may be affected under variable operating conditions. The current study focuses on the analysis of the force–stroke relationship by modifying key excitation parameters such as frequency and amplitude. The tests will be performed for different stroke amplitudes and frequencies ranging from 0.3 Hz to 1 Hz. The experimental setup can be used on either standard or adaptive shock absorbers. It allows for controlled variation of input signals, thus enabling the observation of the dynamic response and how it varies over time. The resulting diagrams provide insights into the energy dissipation process and into the hysteresis phenomenon that occurs while testing. Also, a mathematical model developed in AMESim will be used to compare the results obtained with both experimental and numerical methods. The study contributes to a better understanding of shock absorber behaviour, helping to build a foundation for future developments involving control strategies for adaptive suspension systems.

Keywords: nonlinear viscous damper; excitation frequency; stroke amplitude; hysteresis; AMESim simulation; experimental validation

Academic Editor: Pak Kin Wong

Received: 31 July 2026
Revised: 3 September 2026
Accepted: 3 September 2026
Published: 7 September 2026

1. Introduction

Nowadays, the automotive industry faces an increasing demand for ride comfort and vehicle safety. To satisfy these continuously rising requirements, suspension systems must be designed as efficiently as possible, ensuring an optimal balance between price, comfort, and safety.

It is well known that the oscillatory behaviour found in mechanical systems cannot be properly analysed without considering the damping effect. In automotive suspension systems, the component responsible for the reduction of the wave form is generally a hydraulic damper, which may have a conventional monotube or twin-tube configuration or a more sophisticated design incorporating active or semi-active control capabilities. Regardless of the damper type, its integration into a suspension system requires a comprehensive analysis of its operating parameters, dynamic behaviour, and physical modifications that may occur from long-term operation.

The first stage analysis is the theoretical analysis. A mathematical model can be used to estimate the principal dimensions and operating parameters of the damper before its integration into the suspension system. However, numerical methods alone cannot fully validate the damper's behaviour; thus, experimental investigations should be performed on dedicated test benches, as concluded by the authors of the paper [1].

In addition, to validate the theoretical models, experimental testing has become increasingly important due to continuously growing demand in performance for modern day suspension systems. Another important aspect is that experimental analysis makes it possible to verify whether the damper satisfies the required operating characteristics while also providing valuable information for the optimisation of its kinematic parameters. Following multiple sets of testing, the optimum mounting position of the damper can be determined, for which the suspension would have a better ride comfort and vehicle stability. The authors of paper [2] determined the optimal damper position using the weighted root mean square method, demonstrating that even small variations in mounting position may significantly influence both ride comfort and overall performance of the suspension system.

Hydraulic dampers exhibit inherently nonlinear operating behaviour, as shown by numerous studies, including paper [3] and paper [4], where the authors identified the nonlinear characteristic of hydraulic dampers present in both automotive and civil engineering applications. In practice, the nonlinear behaviour is defined by a difference in compression and rebound strokes. Consequently, the damping coefficient in the rebound phase is generally higher than that during compression, typically satisfying the relationship shown below:

$$\frac{c_{rebound}}{c_{compression}} \cong 2 \tag{1}$$

Results found by Simms and Crolla [5] suggest that a complete characterisation of the damper is essential since simplifying its behaviour by assuming a constant damping coefficient may introduce significant errors in vehicle dynamic simulations. For this reason, the investigated damper will be tested under various operating conditions by varying its piston stroke to simulate different excitation situations and determine different characteristics for each of the cases.

The nonlinear characteristic of the damper evolves over time because of manufacturing quality, hysteresis, and temperature influence.

Therefore, when evaluating damper performance, it is important to consider not only the measured values but also their repeatability. A stable manufacturing process is essential to ensure consistent dynamic behaviour, as highlighted in the paper [6].

This phenomenon becomes visible during long-term operation, leading to gradual modifications in damper parameters. Hysteresis may appear due to delayed valve opening at high piston velocities, friction between the surfaces of the internal components, deformation of valve elements and seals, or the slight compressibility of the hydraulic fluid. Consequently, the damping force depends not only on the instantaneous piston velocity but also on the loading history, contributing to the nonlinear behaviour of the damper [7].

The authors of [8] remarked that after cyclic loading at high force levels, hysteresis effect becomes increasingly evident in both the force–displacement and force–velocity characteristics. The enlargement of the hysteresis loop indicates an increase in the energy dissipated during each loading cycle.

Temperature also has a significant influence on damper performance [9]. As the operating temperature increases, the damping efficiency decreases due to the reduction of the maximum damping force generated during operation. According to the results reported in the paper [10], the maximum damping force decreases by approximately 2 to 9% after the damper reaches the normal operating temperature. The most pronounced force variation can be observed at low piston speed rates, a phenomenon that was also reported by Hryciow in their paper [11]. Thus, the increase in damping force may result in a reduced tire-road contact, leading to a decrease in the EUSAMA coefficient [12].

The modification of the oil viscosity becomes even more critical in the case of magnetorheological dampers, where the change in fluid properties directly influence the damper's behaviour, making active control harder [13]. Consequently, the operating temperature must be continuously monitored and properly controlled to ensure reliable performance, as discussed in [14].

Several theoretical models can also be used to determine the characteristic parameters of the shock absorber.

Mathematical models are developed to describe the dynamic behaviour of the suspension and to predict the characteristic force–displacement and force–velocity relationships of the damper. It is common for these methods to be unable to fully reproduce complex, real, nonlinear characteristics because phenomenon such as hysteresis cannot be fully quantified. The authors of paper [15] demonstrated that the nonlinear damper characteristic can be reasonably approximated using a tangent function that is able to approximate and consider the hysteresis phenomenon. Despite this improvement, theoretical models must still be validated through experimental analysis to ensure the reliability of the predicted results.

The limitations of numerical models become even more evident in the case of magnetorheological dampers and active suspension in general. The authors of [16] reported that accurately approximating both the nonlinear characteristic and the hysteresis behaviour of such dampers remain a significant challenge. Consequently, they also concluded that experimental testing is indispensable for validating numerical predictions and accurately identifying the dynamic parameters of the damper.

A similar conclusion was also made by Tabacu in his Romanian works [17], who emphasised the essential role of experimental testing in validating theoretical models. In that study, a mathematical model based on the Bouc–Wen formulation was developed using experimentally acquired data [18]. Experimental testing represents the fundamental stage in determining the dynamic characteristics of the damper, providing the data required for accurate parameter identification. Compared with simplified suspension representations like the quarter car model, the Bouc–Wen approach offers improved accuracy in reproducing nonlinear damper behaviour.

The quarter car model provides a simplified model of calculus, which can be used with ease for parameter identification when working with passive dampers [19]. The model considers a single wheel assembly together with the corresponding sprung mass, suspension spring, and damping element. It has also been successfully applied to semi-active suspension systems, as demonstrated in paper [1], where the authors remarked that regardless of the mathematical model used, theoretical predictions must always be supported by experimental validation.

However, in the paper [20], the authors argued that the damper cannot be analysed independently, and the analysis of both dampers at once would give more precise results. This suggested that the quarter car model itself is not very precise, indicating that the half-car model offers improved accuracy compared with the quarter car approach. The same concept also applies to experimental routine testing, with good examples of methods used on dampers that are still mounted on the vehicle. One example is the EUSAMA method described in the paper [21], whose authors also pointed out that analysing a single isolated damper may lead to inaccurate conclusions [22].

The work of Worden [23] further supports this perspective by concluding that there is no universally optimal method for damper testing. Instead, theoretical and experimental approaches should be regarded as complementary rather than competing techniques, each providing specific advantages depending on the objectives of the investigation. Consequently, the experimental methodology proposed in this study is not intended to represent the best testing method, but a rather practical, accurate, and repeatable method of producing reliable results suitable for engineering analysis.

Nowadays, research on active and semi-active suspension systems is becoming increasingly widespread, with new technologies being introduced every year. Due to the functional requirements imposed on these systems, nonlinear behaviour remains the defining characteristic of modern dampers. Experimental analysis can be applied not only to conventional hydraulic dampers but also to magnetorheological dampers, solenoid-controlled dampers, and other emerging suspension technologies.

As shown by the previous authors, the nonlinear characteristic of dampers must be thoroughly studied to achieve a better level of understanding of their dynamic behaviour. When it comes to active dampers, this requirement becomes even more important. Consequently, developing accurate mathematical models of such systems remains a significant challenge.

Experimental investigations also play a fundamental role in understanding the real-time variation of the operating parameters of active dampers, as emphasised in [24]. The data obtained from experimental testing are essential for the design, calibration, and implementation of mechatronic control systems capable of regulating the damping force according to the operating conditions [25]. Without reliable experimental data, the development and validation of such control systems would not be possible, as S. Marcu stated in his Romanian works [26].

The investigation of nonlinear behaviour is not limited to conventional active damper technologies. Alternative concepts have also been proposed, including dampers incorporating an elastic slit membrane within the piston assembly. In these systems, the membrane acts as a variable-flow valve, modifying the damping coefficient once the hydraulic pressure reaches a predetermined level. The nonlinear behaviour of this type of damper was investigated by the authors of [27], who combined experimental testing with numerical analysis to validate the results obtained.

Based on the literature review presented above, it can be concluded that experimental testing remains indispensable for the accurate characterisation of automotive dampers. Therefore, the objective of the present work is to develop and validate a dedicated experimental test bench capable of determining the principal damping parameters under controlled operating conditions. The proposed methodology enables the evaluation of the force–displacement and force–velocity characteristics and the identification of nonlinear behaviour and hysteresis effects and provides reliable experimental data for the validation of theoretical models.

2. Materials and Methods

2.1. The Experimental Methods

This paper focuses on the development and application of an experimental test bench featuring a simple, robust design and a simple operating procedure. The proposed methodology was based on experimental analysis using a test bench, in which the damper was removed from the suspension assembly and then mounted on the test rig. The shock absorber was subjected to repeated compression and rebound cycles generated by a mechanism that simulated road surface irregularities. The test bench allowed for the excitation frequency and stroke amplitude to be adjusted, enabling the simulation of various working conditions. To characterise the damper behaviour, force and displacement sensors were employed to continuously measure the damping force and piston displacement throughout the test. The front and rear views of the experimental test bench are presented in Figure 1, together with the principal components of the system.

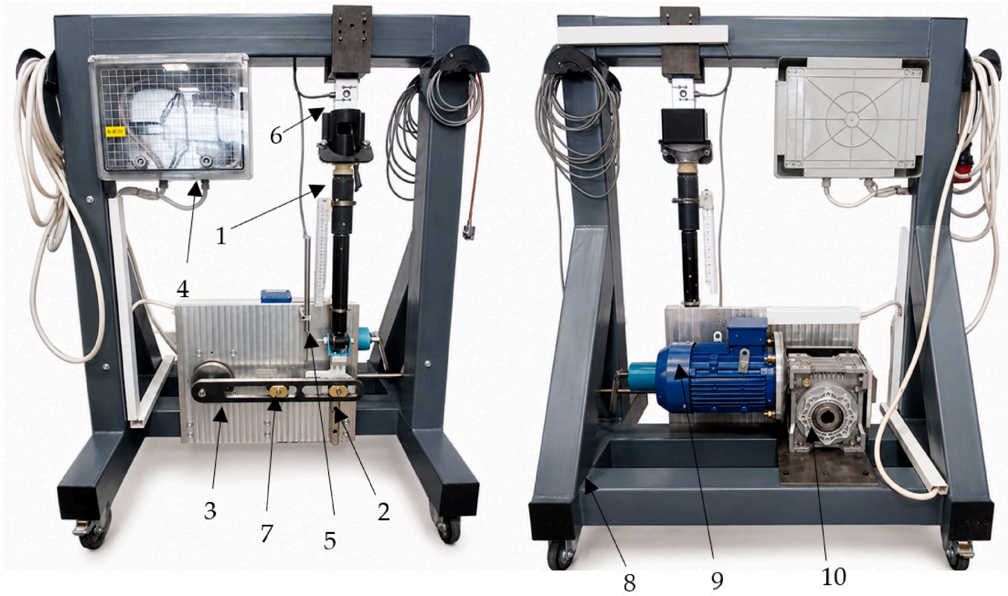

(**a**) (**b**)

Figure 1. The front view of the stand (**a**) and the rear view of the stand (**b**).

Based on the experimental data acquired during testing, the main operating characteristics were determined, namely the force–displacement and force–velocity relationships. Using the measured force and piston velocity, the equivalent damping coefficients for both the compression and rebound phases can be evaluated. Furthermore, the proposed methodology enabled the identification of hysteresis effects through the analysis of the characteristic curves and allowed for the energy dissipated during each operating cycle to be determined. Since the damper was tested independently, the influence of elements such as the suspension spring, tires, and joints was eliminated, resulting in a more accurate characterisation of the damper itself.

The proposed experimental methodology offers significant advantages in terms of accuracy, repeatability, and testing efficiency, allowing for multiple measurements to be completed within a relatively short period of time. This facilitates a more detailed investigation of hysteresis phenomena and the assessment of performance degradation caused by repeated loading cycles. Furthermore, the experimental results can be used to validate mathematical models and provide reliable input data for the optimisation of damper performance as well as for the development of advanced control strategies applicable to active and semi-active suspension systems.

The components presented in the Figure 1 are as follows: 1—tested damper; 2—linkage; 3—rotating crank; 4—variable frequency drive (VFD) control panel; 5—position transducer; 6—force transducer; 7—sliding joint; 8—frame; 9—electric motor; 10—worm gear.

The tested component was an NTY A-AU-009 aftermarket magnetorheological rear shock absorber, corresponding to Audi OE reference 8V0 513 021 E. The damper is intended for installation on either side of the rear axle of selected Audi S3 and RS3 8V vehicles equipped with coil springs and the electronically controlled Audi Magnetic Ride suspension. It is a gas-pressurised damper whose damping force can be adjusted through the application of an electric current to the internal electromagnetic coil, thereby modifying the rheological behaviour of the magnetorheological fluid. Although the damper is designed to permit semi-active damping control, no control current was applied during the present experiments. Consequently, it was operated and evaluated as a passive damper, and all the reported force–velocity characteristics and equivalent damping coefficients correspond to its unenergised state.

The damper's upper section is fixed to the frame. A special mount was designed using 3D scanning to ensure sufficient contact surface between the tested damper and the support. The 3D scan of the upper section of the tested damper, used to design the corresponding mounting support, is shown in Figure 2.

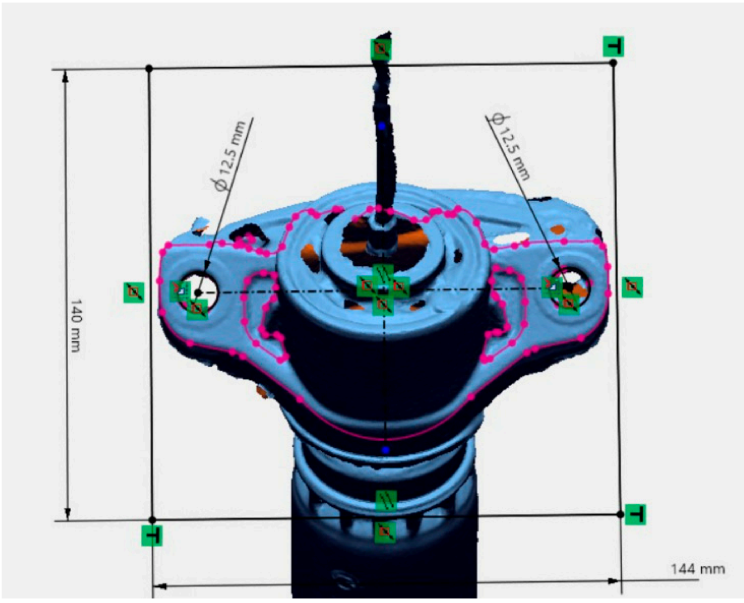

Figure 2. The 3D scan of the upper damper's section.

The lower section of the damper (the piston) is actuated through a linkage that connects it to a rotating crank powered by an electric motor. Because the speed of the motor would be too high for the shock absorber, a worm gear is used to reduce the speed and enhance the maximum momentum.

Motor speed can be manipulated using a variable frequency drive control panel (VFD). The panel allows for precise and stable frequency control, and it is also used to start the electric motor. It has a small liquid-crystal display (LCD) panel that displays the exact frequency in Hz that can be measured at the crank after the worm gear.

To control the stroke amplitude, a sliding joint is used. It can be moved horizontally to modify the stroke of the damper. When moved to the far left, the stroke can reach its maximum value of 72.69 mm. When moved to the far right, the stroke is limited to 42.62 mm. The left-to-right movement of the joint is mechanically limited to 56 mm. A lead screw is used to move the joint and keep it in place. In Figure 3, the joint is positioned all the way to the right at the maximum offset of 56 mm, meaning that the stroke of the shock absorber is 42.62 mm.

To collect data, the stand uses two sensors and a data acquisition unit (DAU).

There is a force sensor on top of the damper made by HBM. The S-shaped S9M load cell can measure the rebound damping force with a precision class of 0.02. It can withstand a maximum of 5 kN, greater than the maximum load capacity of a typical SUV damper.

The second is a position sensor, also produced by HBM. The 1-WA/200MM-L is an inductive, high precision, position sensor that can accurately measure modifications in the vertical position of the shock absorber piston.

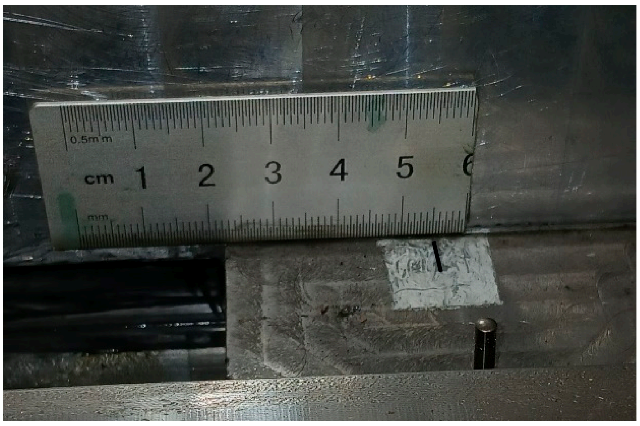

Figure 3. The cursor is used to adjust the sliding joint.

The data acquisition unit represents a key component of the experimental test bench. It collects data from both sensors in real time. It correlates and synchronises the force and piston position at any given time, enabling the determination of the damper's characteristics. Using dedicated software, the piston displacement and time can be transformed in piston speed; thus, a force–velocity characteristic can be created. The relationship between force and velocity can be described by the following formula:

$$F_d = c(v_d) \cdot v_d \tag{2}$$

$$where\ c(v_d) = \begin{cases} \sum\limits_{i=1}^{n} a_{i,c} \cdot {v_d}^{i-1},\ v_d < 0\ compression \\ \sum\limits_{i=1}^{n} a_{i,r} \cdot {v_d}^{i-1},\ v_d > 0\ rebound \end{cases}$$

where $a_{i,c}$ and $a_{i,r}$ are polynomial coefficients identified from the experimentally measured force–velocity data.

Furthermore, the acquired data can be stored, processed, and exported into other software programs, like Excel.

2.2. The Mathematical Model

To verify the experimental results, another model must be used. The model in question was a custom mathematical model that resembled the testing bench. The Amesim simulation software developed by Siemens was used to simulate the parameters of the numerical model. The numerical simulations were performed using LMS Imagine.Lab AMESim 12.0.0 Rev 12 software. The model contained the shock absorber, which was the main component, and two sensors that represented the actual sensors used for the experimental bench, one in the top of the damper for measuring the force and the other on the opposite side of the damper, which was used to measure the displacement. The data collected from the two sensors was sent to a two-input signal writer that automatically created a document containing the collected data. The upper end of the damper was connected to a "zero-speed source", thereby imposing a fixed boundary condition consistent with the experimental test-bench configuration. A sinusoidal displacement signal was applied to the lower end of the damper to reproduce the excitation imposed by the experimental test bench.

In addition, a linear velocity sensor measured the velocity of the lower end of the damper transmits this signal to a one-dimensional lookup table. Based on the measured velocity, the table determined the corresponding damping coefficient through interpolation and supplied it to the variable-damping input of the damper model. The tabulated velocity–damping-coefficient characteristic can be modified for any investigated damper using data obtained experimentally or provided by the damper manufacturer. This approach enabled the model to reproduce the velocity-dependent and asymmetric behaviour of the damper during the compression and rebound strokes.

The interpolation table is considered valid within the velocity range covered by the input data. Else, AMESim will not be able to compute a simulation.

Some of these components required input parameters. The signal source was a sinusoidal one with the frequency equal to the frequency of the crank used in the experimental model. The tire's elasticity and mass was neglected.

The AMESim model used for the numerical analysis is shown in Figure 4.

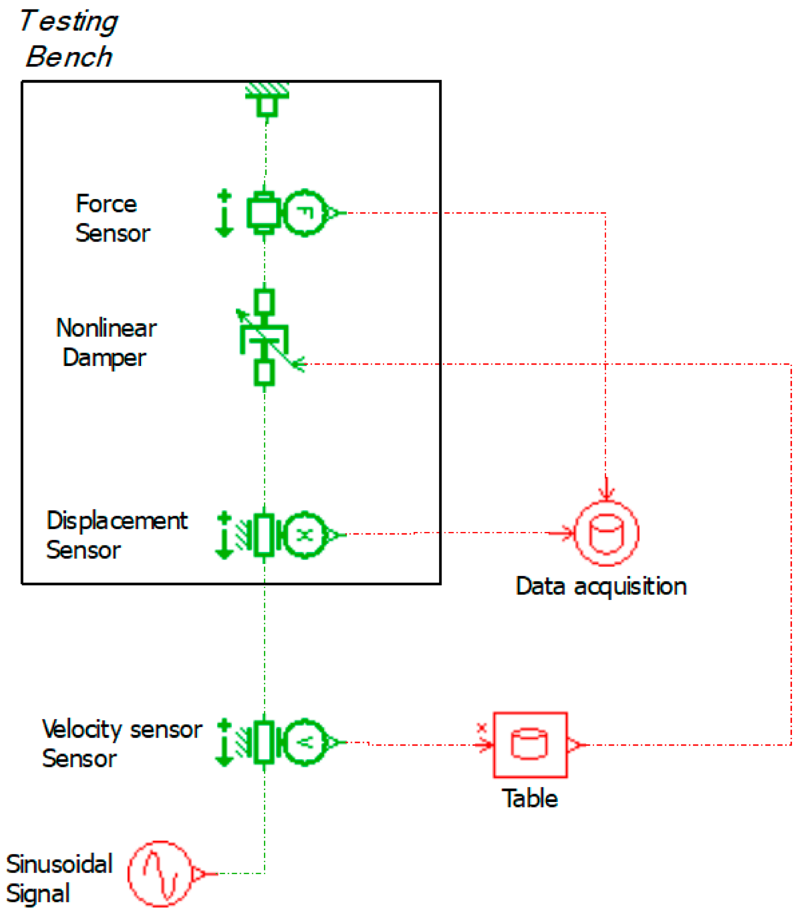

Figure 4. The custom model developed in AMESim. Green solid lines and icons represent the mechanical domain (force, displacement and velocity sensors, nonlinear damper model and testing bench), while red dashed lines and icons represent the signal/control domain (sinusoidal excitation, table and data acquisition).

AMESim allows the parameters of a numerical model to be defined either using user-specified values or data obtained from experimental measurements. In the first approach, the model components are characterised by constant or predefined parameters, such as mass, stiffness, and damping coefficients. Alternatively, experimentally determined characteristics, such as the force–velocity curve of a damper, can be introduced as tabulated datasets and used by the software to describe the component behaviour through interpolation. In the Results chapter, experimental and mathematical methods will be compared for cases with same excitation parameters as inputs (frequency and amplitude). The AMESim model will require no extra parameters to be declared. The calculation procedure begins with the definition of the excitation amplitude (A) and frequency (f). Unlike a quarter-car configuration, the revised numerical model directly reproduces the boundary conditions of the experimental test bench. The upper mounting point of the damper is fixed by means of a zero-speed source; therefore, the sinusoidal displacement signal cand be quantified with the following formula:

$$z_L(t) = A \cdot sin(2\pi f t) \tag{3}$$

The program then calculates the velocity using derivation, the variable being time (t):

$$\dot{z_L}(t) = 2\pi f \cdot A \cdot cos(2\pi f t) \tag{4}$$

where L stands for "lower end of the damper", f is the frequency, A is the maximum amplitude, and t is time.

The damping force formula used by AMESim is the same as formula as (2):

$$F_d = c(v_d) \cdot v_d$$

Please note that the displacement and velocity formula apply only for the lower end of the damper, the upper one being fixed.

$$z_U = 0$$
$$\dot{z}_U = 0$$

where U stands for "upper end of the damper".

The relationship between the damping coefficient and the relative velocity was determined in AMESim by interpolating between the experimentally derived velocity–damping-coefficient data pairs provided in the one-dimensional lookup table. The implementation of the experimental dataset in the one-dimensional lookup table required extensive pre-processing since the measured data contained repeated velocity values, local fluctuations, and several anomalous points. According to the sign convention adopted in the present model, the measurements were first divided into two datasets: negative relative velocities corresponding to the compression phase and positive relative velocities corresponding to the rebound phase. The initially obtained velocity–damping-coefficient data are presented in Figure 5.

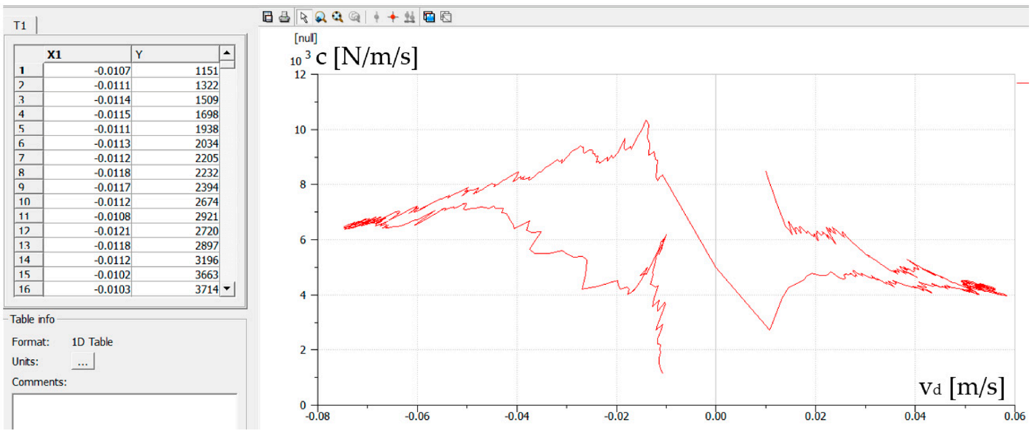

Figure 5. An example for an experimentally acquired characteristic.

Subsequently, the velocity values were arranged in ascending order, while duplicate entries were consolidated by averaging their corresponding damping coefficients, resulting in the characteristic shown in Figure 6.

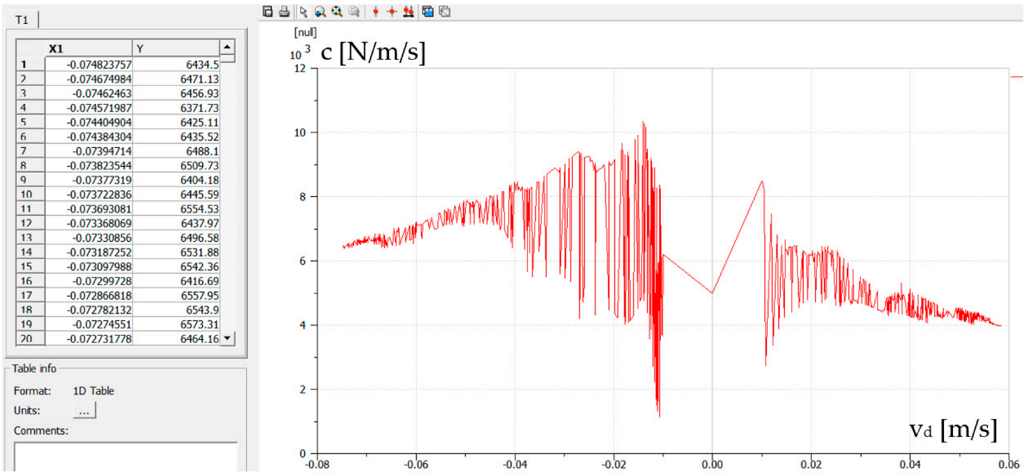

Figure 6. The resulting characteristic after arranging the data.

To reduce the influence of experimental outliers, the velocity range was divided into equal-width intervals, and the median damping coefficient was calculated for each interval. A robust third-degree polynomial regression based on the Huber loss function was then applied to the binned median values, producing a smooth and continuous nonlinear relationship between the damping coefficient and relative velocity. Microsoft Excel was used for data organisation, visualisation, calculation, and implementation of the polynomial formula. The result can be seen in Figure 7.

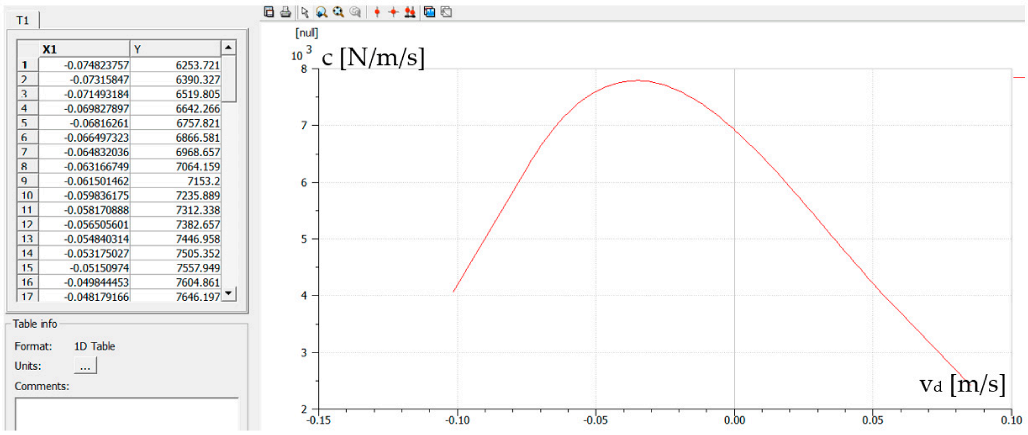

Figure 7. The final, smooth, and continuous c = f(v_d) characteristic.

3. Results

3.1. The Experimental Model

3.1.1. Constant Frequency

In the first set of measurements, the characteristics of the damper will be compared for a fixed frequency of 0.3 Hz and different values for the maximum amplitude. The crank will be exactly 30 rpm. Three tests were performed for the given frequency.

1. Sliding joint in the neutral position (cursor at 10 mm);
2. Joint shifted 18 mm to the right;
3. Joint fully shifted to the right (cursor at 56 mm).

The temperature will be considered and will be maintained at 24 °C across all bench tests, with cooling pauses allocated between runs. Hysteresis effects were evaluated prior to the final tests to ensure that components such as the test bench joints did not contribute to parasitic hysteresis.

Each test lasted 20 s, and the DAU logged data every 3.33 ms.

After all the three tests, the results are compiled in two characteristics showing the dependence between force–displacement and force–velocity.

In Figure 8, the force-displacement characteristics is shown for three different damper strokes. The force and displacement are parameters measured directly on the test bench.

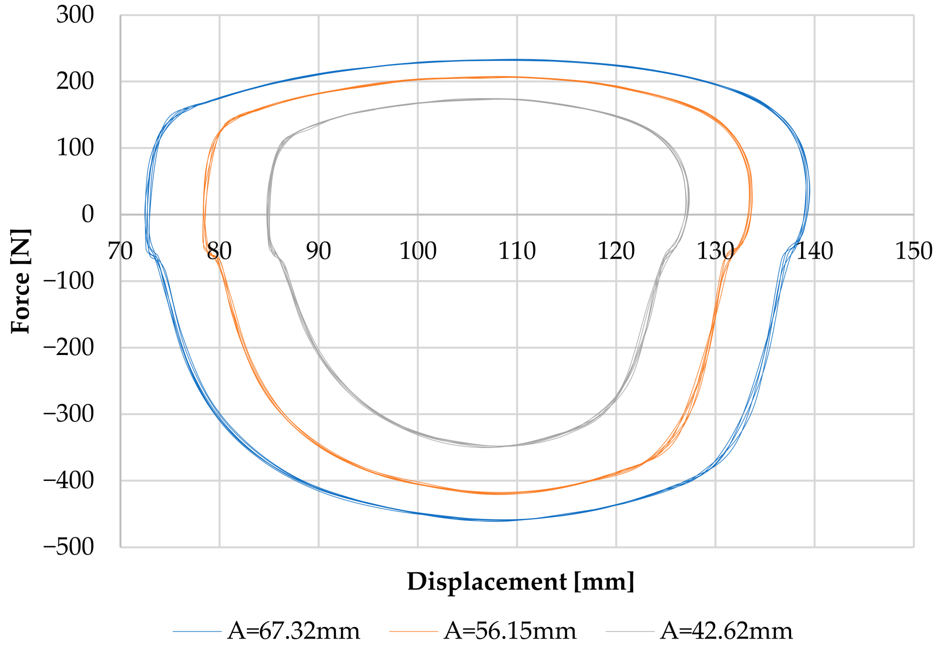

Figure 8. The force–displacement characteristic.

As shown in Figure 9, the force–velocity characteristics obtained at different excitation amplitudes exhibit similar overall trends. However, the relationship between damping force and piston velocity is not strictly linear, and therefore, the damping coefficient cannot be regarded as a universal constant. For each test condition, an equivalent mean damping coefficient was determined by applying the least-squares method to the corresponding experimental data.

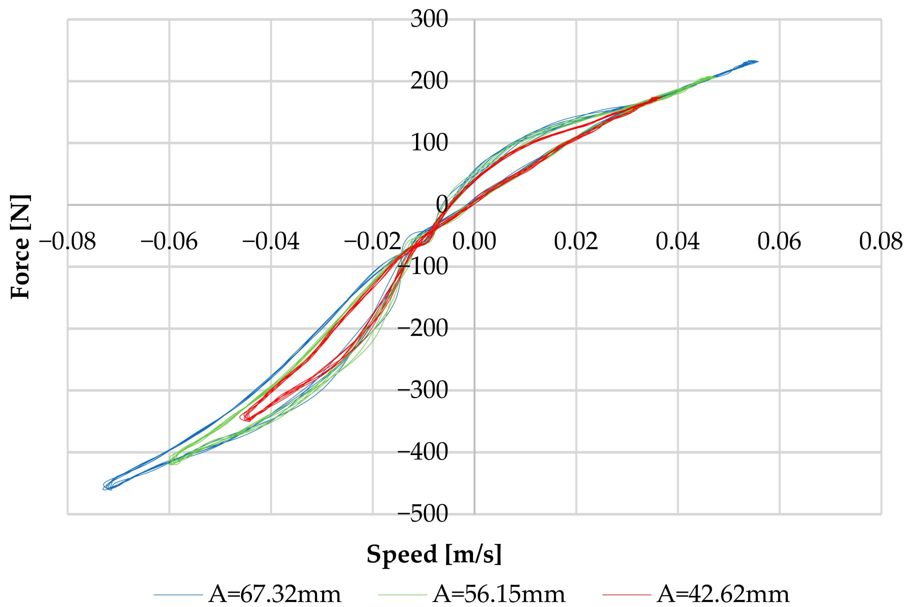

Figure 9. The force–velocity characteristic.

The formula used for the coefficient using the least-squares method is:

$$c = \frac{\sum v_{id} \cdot F_{id}}{\sum v_{id}^2} \quad (5)$$

The experimental force–velocity data were divided into two datasets according to the direction of piston motion. The least-squares equation was then implemented directly in Microsoft Excel and applied independently to the compression and rebound datasets to determine the corresponding equivalent mean damping coefficients, c_c and c_r, respectively.

The resulting coefficients varied only moderately with excitation amplitude, from $c_r = 6634\frac{N \cdot s}{m}$ for the rebound phase and $c_c = 4452\frac{N \cdot s}{m}$ for the compression phase for a stroke of $A = 67.32$ mm to $c_r = 7506\frac{N \cdot s}{m}$ for the rebound phase and $c_c = 4922\frac{N \cdot s}{m}$ for the compression phase for stroke of $A = 42.62$ mm. This variation confirms that the damper behaviour is dependent on the operating conditions. A perfect constant coefficient cannot be determined because the characteristic is nonlinear. However, the following relation between the two coefficients can be written.

$$\frac{c_{rebound}}{c_{compression}} = \frac{7506}{4922} = 1.525$$

3.1.2. Same Maximum Amplitude

The second set of measurements was performed by maintaining a constant maximum stroke of 67.32 mm across four different frequencies: 0.3 Hz, 0.5 Hz, 0.7 Hz, and 1.0 Hz.

In the case of a constant maximum stroke, the damping force increases with the frequency as demonstrated in Figure 10.

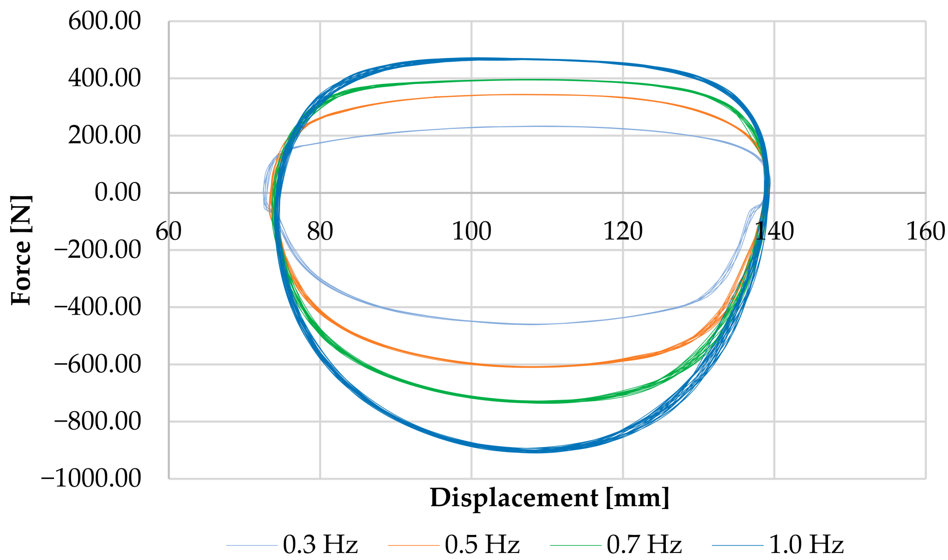

Figure 10. The force–displacement characteristic.

In Figure 11, when the frequency increases, both force and speed increase. However, in this case, the damping coefficient is different. In this case of frequency increasing from 0.3 Hz to 1.0 Hz, the rebound damping coefficient decreases from 6874 Ns/m to 3889 Ns/m. The same modification applies for the compression coefficient too.

https://doi.org/10.3390/vehicles8090214

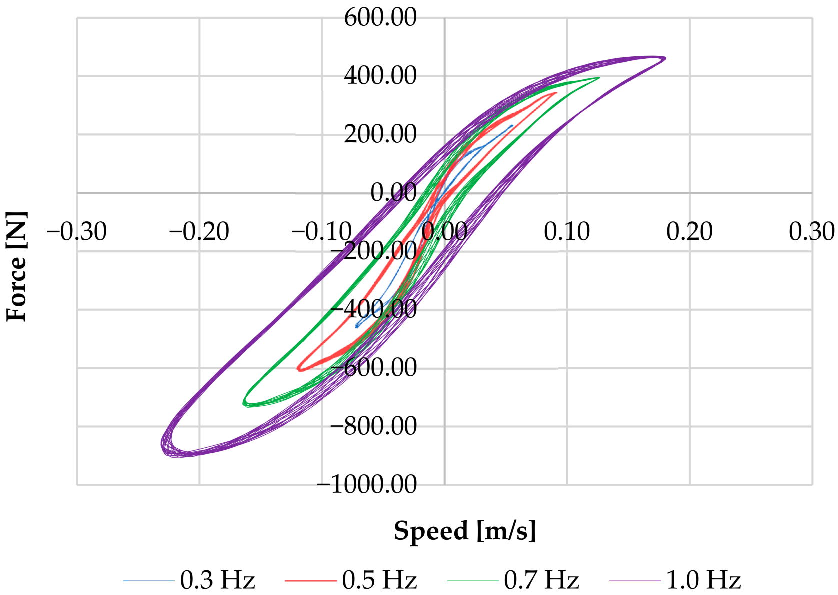

Figure 11. The force–velocity characteristic.

A table with each damping coefficient can be created:

Using Table 1, the following characteristic can be created:

Table 1. Damping coefficients for different frequencies.

Frequency	Compression Coefficient	Rebound Coefficient
0.3 Hz	4452 Ns/m	6634 Ns/m
0.5 Hz	3980 Ns/m	5460 Ns/m
0.7 Hz	3369 Ns/m	4676 Ns/m
1 Hz	2728 Ns/m	4016 Ns/m

Figure 12 shows that the apparent damping coefficient decreases with increasing excitation frequency. The variation is not linear but exhibits a smooth curvilinear trend, with a steeper decrease at low frequencies followed by a gradual stabilisation at higher excitation frequencies. This behaviour reflects the nonlinear hydraulic characteristics of the damper and confirms that the damping coefficient cannot be considered constant over the entire operating range.

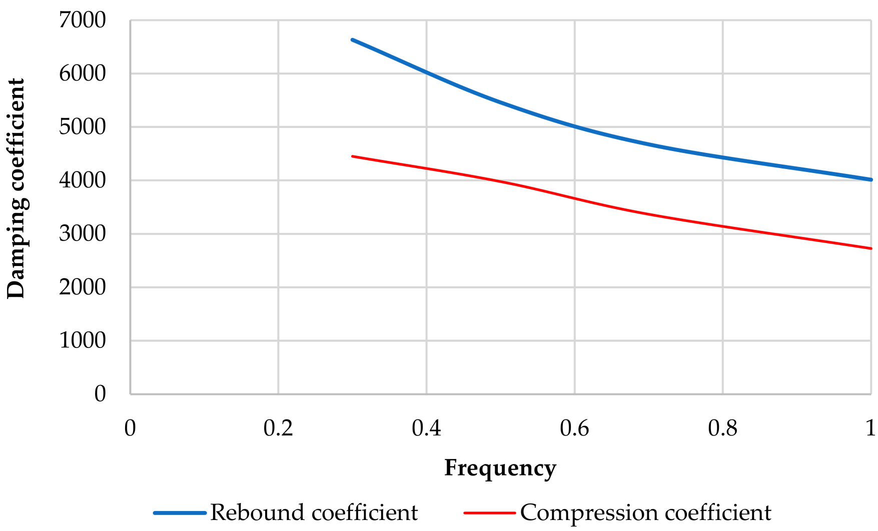

Figure 12. Damping coefficient variation over frequency.

Although the obtained results indicate a clear trend, additional experimental measurements over a wider range of operating conditions are required to draw more robust conclusions.

3.1.3. Displacement, Force, and Speed Variation over Time

The comparison is made between two tests, one performed at 1 Hz and the other at 0.3 Hz. Both have the same maximum stroke of 67.32 mm. The following characteristics can be analysed:

Analysing the graph in Figure 13, it is evident that the maximum displacement amplitude remains constant and equal regardless of frequency.

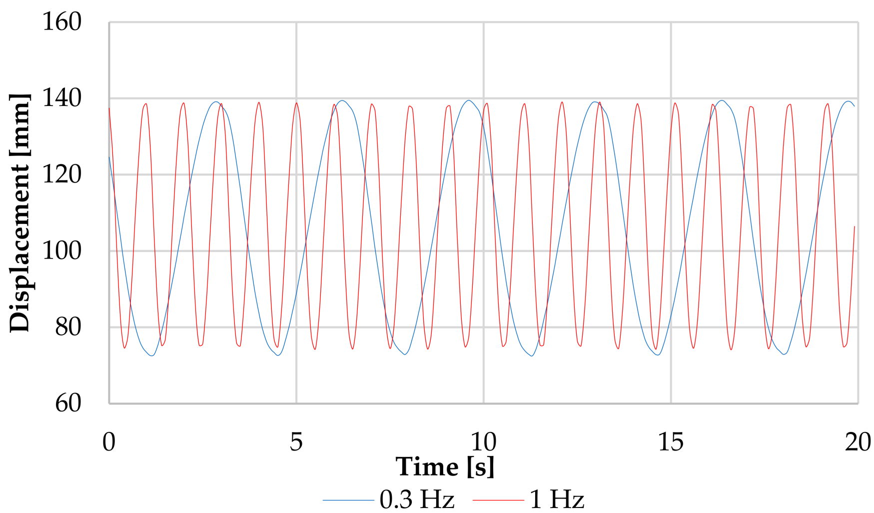

Figure 13. Displacement variation over time for various values of frequency.

Analysing the graph in Figure 14 shows that the considerable increase in the maximum damping force at 1 Hz compared to 0.3 Hz. Since the stroke amplitude remains constant, the increase in force is mainly attributed to the higher piston velocity, which is directly proportional to the excitation frequency.

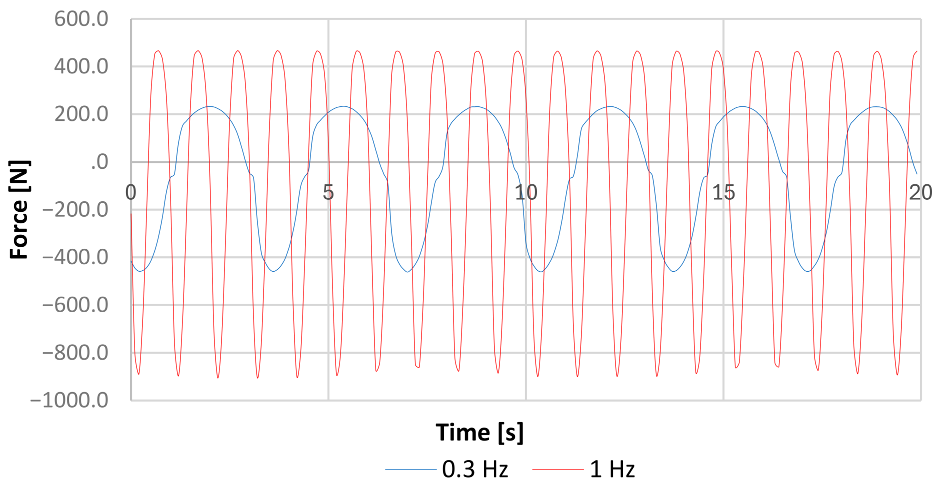

Figure 14. Force variation over time for various values of frequency.

As shown before in Formula (2), the force is proportional with the speed of the damper. Furthermore, the speed–time variation and force–time will exhibit the same trend, but with the damping coefficient changing the maximum amplitude, as shown in Figure 15.

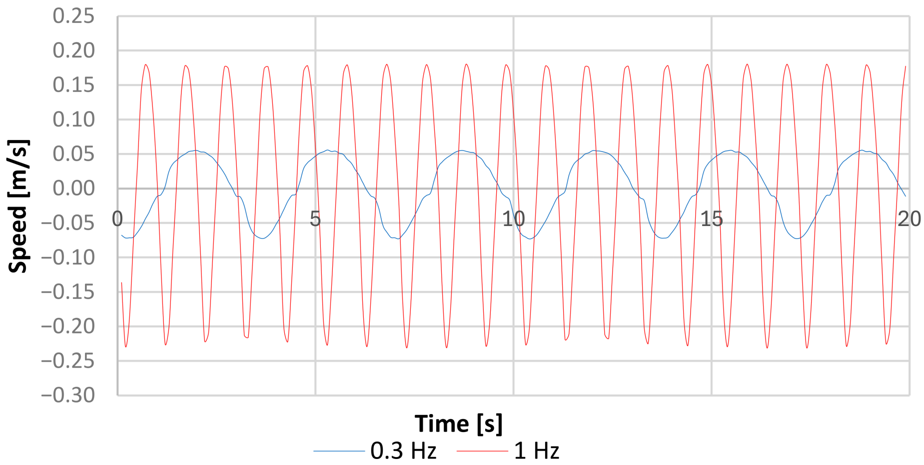

Figure 15. Speed variation over time for various values of frequency.

A second set of tests will be conducted at different maximum amplitudes while maintaining a constant frequency. The set frequency is 0.3 Hz. The displacement, damping force, and piston velocity time histories obtained at constant frequency and different excitation amplitudes are presented in Figures 16–18, respectively.

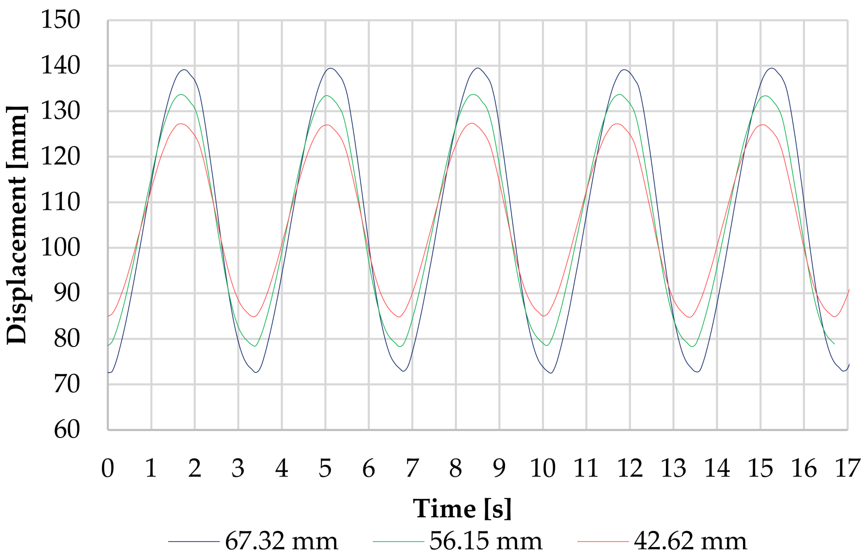

Figure 16. Displacement variation over time for different values excitation amplitudes.

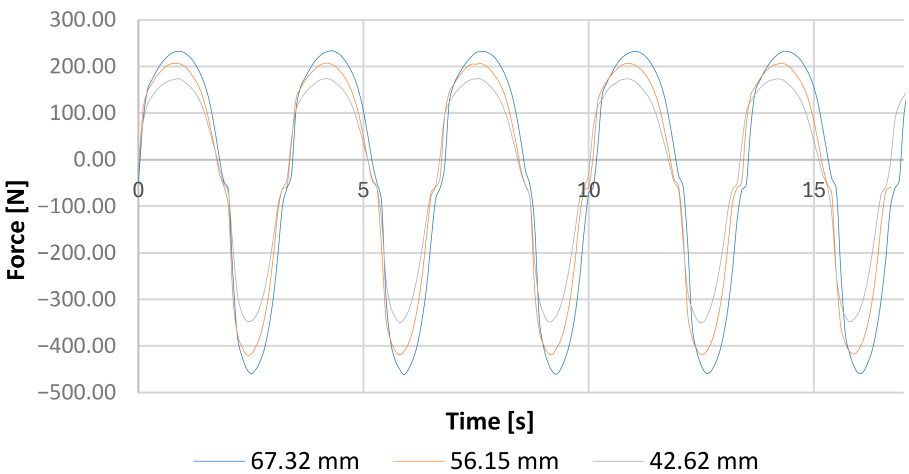

Figure 17. Force variation over time for different values excitation amplitudes.

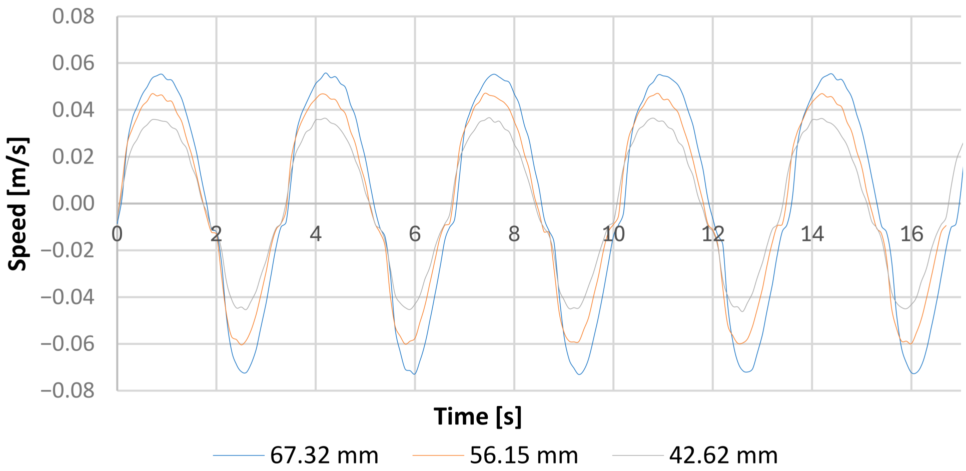

Figure 18. Speed variation over time for different values excitation amplitudes.

Although different excitation amplitudes were applied, all displacement and force signals exhibit a similar overall shape, indicating that the damper maintains the same operating principle throughout the investigated stroke range. The increase in amplitude mainly affects the magnitude of the response rather than its overall waveform.

Figure 17 shows that increasing the excitation amplitude results in higher peak damping forces. As well as in the characteristics in the Figures 14 and 15, Figures 17 and 18 show the same bond between the force and speed provided by the damping coefficient.

The hysteresis observed in the force–velocity diagrams are indicated by the occurrence of different damping-force values at the same piston velocity, depending on whether the piston is accelerating or decelerating. This behaviour can be attributed to the phase delay between piston motion and pressure development inside the damper. Fluid compressibility, the presence of entrained gas, the finite response time and elastic deformation of the valve elements, and friction at the piston rod and seals may all contribute to this delay. Therefore, the damping force depends not only on the instantaneous piston velocity but also on the previous state of the system.

The experimental curves also indicate that the size and shape of the hysteresis loop vary with the excitation conditions. Increasing the excitation amplitude or frequency changes the maximum piston velocity and the rate at which the internal pressure develops, thereby affecting the valve response and the enclosed loop area. The observed behaviour confirms that a single constant damping coefficient cannot fully describe the tested damper. Consequently, the compression and rebound characteristics were processed separately, and condition-dependent equivalent mean damping coefficients were determined using the least-squares method.

Although these mechanisms provide a physically consistent interpretation of the experimental curves, their individual contributions cannot be quantified from the external force and displacement measurements alone.

To have a better view of the hysteresis phenomenon, a longer experimental test was conducted. A section from the force–displacement characteristic can be seen below.

During the three-minute cyclic test performed at an excitation frequency of 0.5 Hz, approximately 90 loading cycles were recorded. As shown in Figure 19, the individual trajectories do not overlap perfectly but form a relatively narrow band. This cycle-to-cycle separation indicates that the damping force is not determined exclusively by the instantaneous piston velocity, being also influenced by the previous state of the damper.

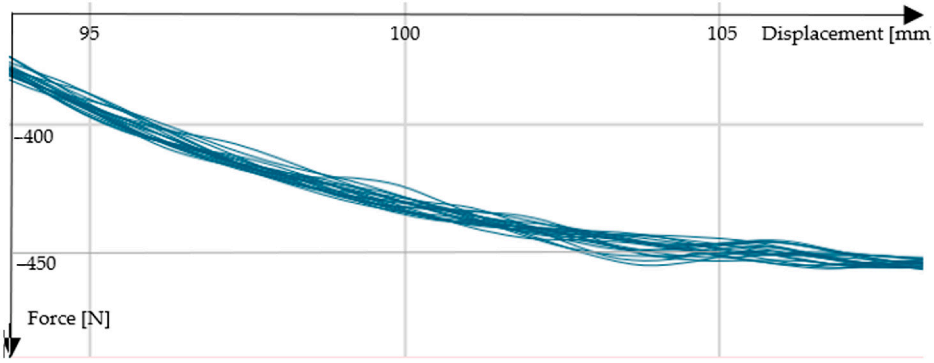

Figure 19. The force and displacement variation over a longer period of testing.

3.2. The Mathematical Method

The parameters used for the first experimental bench test will be used also used for the numerical model. The frequency will be 0.3 Hz, and the maximum stroke will be 67.32 mm. The test also lasts 20 s with a print interval of 3.33 ms. To truly replicate the nonlinear behaviour, a data set collected through experimental analysis is used.

For this simulation, a new c = f(v_d) function was created. The data was gathered from experiments conducted on the real NTY shock absorber at a constant 0.3 Hz frequency. After excel ordination and calculus using the Huber method, the function was obtained. The characteristic used in this experiment can be seen in Figure 7, where it was used as an example to describe the method.

A simulation was started with the excitation parameters listed in Figure 20. The dynamic controlled write component saved all the output parameters such as force and displacement. A direct comparison between the characteristics of the experimental method and numerical method is shown below:

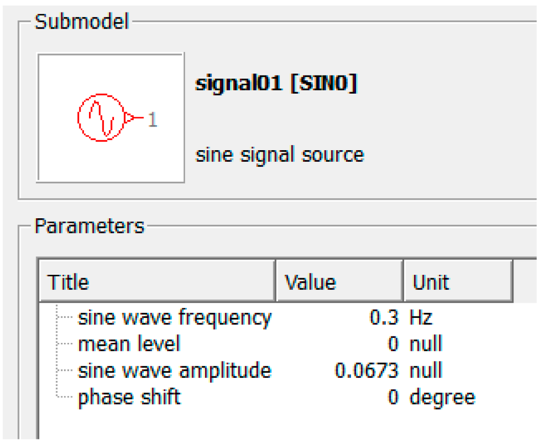

Figure 20. The parameters are introduced in the sinusoidal signal generator.

The experimental and numerical force–displacement characteristics are compared in Figure 21. Although the same nominal sinusoidal displacement amplitude was applied, the piston stroke obtained in AMESim was slightly larger than the experimentally measured stroke. Despite this difference, the numerical and experimental maximum and minimum damping-force values were generally close. Figure 22 compares the corresponding force–velocity characteristics. Both results demonstrate a nonlinear relationship between damping force and piston velocity. However, whereas the experimental characteristic exhibits a visible hysteresis loop, the numerical result follows a single smooth curve and does not reproduce the separation between the hysteresis branches.

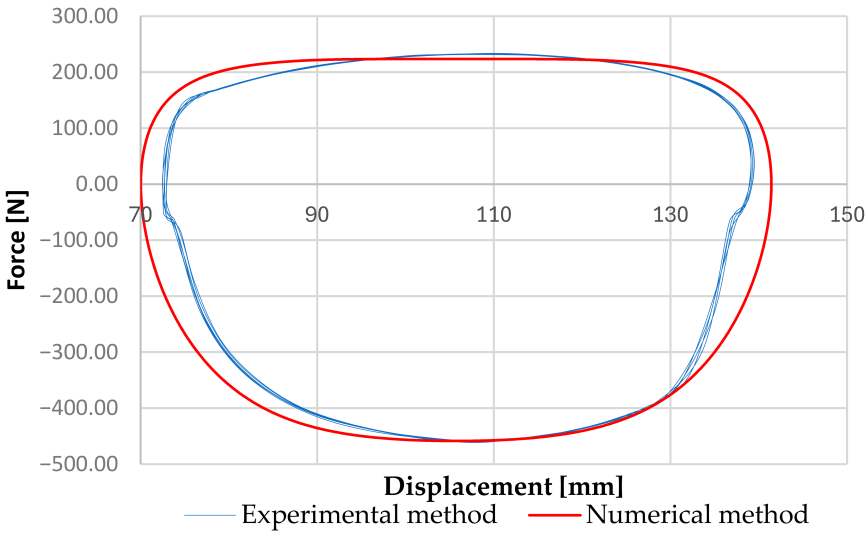

Figure 21. Comparison of force–displacement characteristic.

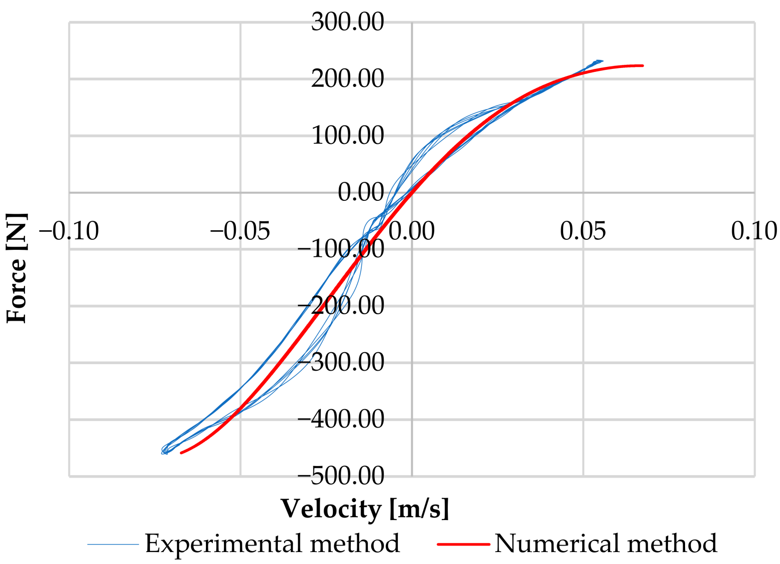

Figure 22. Comparison of force–velocity characteristic.

4. Discussion

The first aspect to be discussed is that, as shown in previous papers, the actual characteristic of a hydraulic damper is inherently nonlinear. Consequently, the damping coefficient cannot be considered constant but varies according to the operating conditions. The compression damping coefficient is smaller than the rebound damping coefficient as shown in Section 3.1.1. This behaviour results from the internal hydraulic valve design, which intentionally provides a higher damping coefficient during the rebound stroke to improve vehicle stability. Another point requiring consideration is that changes in frequency will affect the piston speed and indirectly the maximum rebound force of the damper, the maximum amplitude remaining the same. However, the piston speed increases with the frequency, as shown in the formula below.

$$v(t) = 2 \cdot \pi \cdot f \cdot A \cdot \cos(2 \cdot \pi \cdot f \cdot t)$$

where f is the frequency and A is the amplitude.

The experimental results show that frequency and amplitude influence different aspects of the damper response. Compared to constant maximum amplitude and a constant frequency, increasing the stroke amplitude also produces higher piston velocities and peak damping forces, while the overall waveform remains similar. For this reason, the two excitation parameters should not be analysed independently since their combined effect determines the piston velocity and, thus, the resulting damping force. Nevertheless, the decrease in the apparent damping coefficient observed at higher frequencies confirms that the force response cannot be explained exclusively by the increase in piston velocity and reflects the nonlinear behaviour of the hydraulic damper.

In Figure 11, it can be noticed that the characteristic is not very smooth, especially the shape of the 1 Hz test. The irregular shape of the characteristic curve is attributed to the hysteresis phenomena occurring within the hydraulic damper, although mathematical models cannot fully recreate the complex nonlinear behaviour of real hydraulic dampers and should therefore be regarded as an indicative characteristic of a real damper. Nevertheless, when calibrated using experimental data, they provide valuable estimates of damper behaviour and serve as an effective means of validating the consistency of experimental measurements. The relative error between the experimental and numerical method can be simply quantified as the difference between the maximum force and the maximum speed. In these cases, the errors will be as follows:

$$err = \frac{F_{\max\_r} - F_{\max\_s}}{F_{\max\_r}} \cdot 100\% = 5.1\% \tag{6}$$

$$err = \frac{v_{\max\_r} - v_{\max\_s}}{v_{\max\_r}} \cdot 100\% = 11.24\% \tag{7}$$

Both force and velocity are estimated with good accuracy, even though the velocity's error is a bit higher. This behaviour is expected because the piston velocity is determined mainly by the excitation kinematics, whereas the damping force is strongly influenced by nonlinear hydraulic phenomena that are difficult to reproduce numerically. Consequently, experimental testing and mathematical modelling should be considered complementary approaches, combining the accuracy of direct measurements with the predictive capabilities of numerical simulation.

The slightly larger numerical piston stroke may be attributed to the ideal displacement imposed by the numerical source, while the motion generated by the experimental test bench can be affected by mechanism clearances, structural compliance, and displacement-sensor uncertainty. The close agreement between the maximum and minimum force values indicates that the model adequately reproduces the overall damping-force level. Nevertheless, its ability to describe the internal dynamic behaviour of the damper remains limited. The absence of hysteresis in the numerical force–velocity characteristic is primarily caused by the memoryless one-dimensional relationship $c = c(v)$, which assigns a unique damping coefficient to each relative-velocity value. Furthermore, the robust cubic regression based on the Huber loss function smooths the experimental data and reduces the influence of outliers, but it also eliminates the distinction between the loading and unloading branches. Therefore, the present model reproduces the nonlinear velocity dependence and the compression–rebound asymmetry, but it cannot fully describe the history-dependent behaviour of the practical damper.

As a next step, additional measurements involving different shock absorbers, wider frequency and amplitude ranges, and variable operating temperatures are required to further validate the experimental methodology and the numerical model.

https://doi.org/10.3390/vehicles8090214

5. Conclusions

The present study investigated the influence of excitation frequency and stroke amplitude on the dynamic behaviour of a hydraulic damper using a dedicated experimental test bench. The simple method enabled the controlled modification of the excitation parameters and, consequently, the damping force, displacement, and piston velocity signals required to determine the force–displacement and force–velocity characteristics. The experimental results were subsequently compared with a theoretical model, developed in AMESim. The results confirmed the inherently nonlinear behaviour of the hydraulic damper and showed that the rebound damping coefficient was higher than the compression damping coefficient throughout the investigated operating range. At a constant maximum amplitude, increasing the excitation frequency resulted in higher piston velocities and peak damping forces, while the apparent damping coefficients decreased. The rebound damping coefficient decreased from 6557 Ns/m at 0.3 Hz to 3889 Ns/m at 1.0 Hz, while the compression damping coefficient decreased from 4554 Ns/m to 2696 Ns/m. At a constant frequency, increasing the stroke amplitude also resulted in higher piston velocities and damping forces without significantly changing the overall waveform of the measured signals. The irregularities observed in the characteristic curves also highlighted the influence of hysteresis on the real behaviour of the damper. The comparison between the experimental and numerical results indicated good agreement for the investigated operating condition, with relative errors of 5.1% for the maximum damping force and 11.24% for the maximum piston velocity. Therefore, the data obtained from experimental testing provide valuable information for parameter identification, mathematical model validation, and the optimisation of suspension performance.

The revised AMESim model provides a satisfactory representation of the global nonlinear damping characteristic and predicts force extrema comparable to those measured experimentally. However, the comparison also demonstrates that a one-dimensional velocity-dependent damping-coefficient table is insufficient to reproduce the experimentally observed hysteresis. Future work should therefore consider separate loading and unloading characteristics, a two-dimensional relationship such as ($c = c(v, x)$), or a phenomenological hysteresis model. Additional improvements could be obtained by imposing the experimentally measured displacement signal directly and by accounting for fluid compressibility; seal friction; valve dynamics; temperature; and, when the magnetorheological damper is operated in its controllable mode, the applied control current.

Further investigations should extend the measurements to wider frequency and amplitude ranges, variable operating temperatures, and different types of shock absorbers. An endurance test may be performed on the damper in future tests to show the modifications of the characteristics. In the future, the increasing adoption of semi-active and active suspension systems will require more advanced experimental methods capable of supporting the development of real-time control strategies and adaptive damping characteristics. Consequently, experimental testing will continue to play a fundamental role in the development, validation, and optimisation of next-generation intelligent suspension systems.

Author Contributions: Conceptualisation, G.B., A.D., V.-C.M., and R.-A.D.; methodology, G.B., A.D., V.-C.M., and R.-A.D.; software, G.B., A.D., V.-C.M., and R.-A.D.; validation, G.B., A.D., V.-C.M., and R.-A.D.; formal analysis, G.B., A.D., V.-C.M., and R.-A.D.; investigation, G.B., A.D., V.-C.M., and R.-A.D.; resources, G.B., A.D., V.-C.M., and R.-A.D.; data curation, G.B., A.D., V.-C.M., and R.-A.D.; writing—original draft preparation, G.B., A.D., V.-C.M., and R.-A.D.; writing—review and editing, G.B., A.D., V.-C.M., and R.-A.D.; visualisation, G.B., A.D., V.-C.M., and R.-A.D.; supervision, A.D.; project administration, A.D.; funding acquisition, A.D. All authors have read and agreed to the published version of the manuscript.

Funding: The APC was funded by the National University of Science and Technology POLITEHNICA Bucharest from its own funds.

Data Availability Statement: The data presented in this study are available upon request from the corresponding author.

Acknowledgments: This work was supported by a grant from the National Program for Research of the National Association of Technical Universities—GNAC ARUT 2023.

Conflicts of Interest: The authors declare no conflicts of interest.

References

1. Mei, Y.; Wang, R.; Ding, R.; Jiang, Y. Classification Evolution, Control Strategy Innovation, and Future Challenges of Vehicle Suspension Systems: A Review. *Actuators* **2025**, *14*, 485. [CrossRef]
2. Yin, C.; Liu, Y.; Zhang, J.; Yuan, H.; Wang, B.; Zhang, Y. Research on Optimization and Matching of Cab Suspension Systems for Commercial Vehicles Based on Ride Comfort. *Vehicles* **2026**, *8*, 15. [CrossRef]
3. Maljković, M.; Blagojević, I.; Popović, V.; Stamenković, D. Impact of the Damper Characteristics on the Behavior of Suspension System and the Whole Vehicle. *J. Appl. Eng. Sci.* **2018**, *16*, 349–357. [CrossRef]
4. Dong, B.; Sause, R.; Ricles, J.M. Modeling of Nonlinear Viscous Damper Response for Analysis and Design of Earthquake-Resistant Building Structures. *Bull. Earthq. Eng.* **2022**, *20*, 1841–1864. [CrossRef]
5. Simms, A.; Crolla, D. The Influence of Damper Properties on Vehicle Dynamic Behaviour. In Proceedings of the SAE World Congress, Detroit, MI, USA, 4–7 March 2002; SAE Technical Paper 2002-01-0319. [CrossRef]
6. Stembalski, M.; Ręczkowski, S.; Szydłowski, T. Influence of Shock Absorber Construction on Production Parameters of Its Prototype Solutions. *Appl. Sci.* **2025**, *15*, 12567. [CrossRef]
7. Zheng, X.; Sun, Y.; Zhou, H. Study of the Dynamic Model and Vibration Performance of Pot-Shaped Metal Rubber. *Materials* **2022**, *15*, 5878. [CrossRef] [PubMed]
8. Dithurson, T.; Daniel, C.; Sharma, S.V.; Hemalatha, G.; Nair, S.R.; Solomon, A.A. Experimental Investigation of High-Force-to-Volume Extrusion Damper Subjected to Cyclic and Time History Loading. *J. Appl. Eng. Sci.* **2023**, *13*, 183–188. [CrossRef]
9. Hryciów, Z. An Investigation of the Influence of Temperature and Technical Condition on the Hydraulic Shock Absorber Characteristics. *Appl. Sci.* **2022**, *12*, 12765. [CrossRef]
10. Stembalski, M.; Czarnuch, A.; Szydłowski, T.; Batory, D. Assessment of the Possibility of Validating the Durability Testing Method for Large-Sized Vehicles Based on Changes in Shock Absorber Characteristics—Preliminary Tests. *Appl. Sci.* **2024**, *14*, 127. [CrossRef]
11. Hryciów, Z.; Rybak, P.A.; Gieleta, R. The Influence of Temperature on the Damping Characteristic of Hydraulic Shock Absorbers. *Eksploat. I Niezawodn.—Maint. Reliab.* **2021**, *23*, 346–351. [CrossRef]
12. Żuśka, A.; Jackowski, J. Influence of Changes in Stiffness and Damping of Tyre Wheels on the Outcome of the Condition Assessment of Motor Vehicle Shock Absorbers. *Energies* **2023**, *16*, 3876. [CrossRef]
13. Wu, X.; Chen, Y.; Zhang, Z. Preparation and Performance Evaluation of a High Temperature Stable Magnetorheological Fluid with Shear-Thinning Resistance. *Materials* **2025**, *18*, 3840. [CrossRef] [PubMed]
14. Jastrzębski, Ł.; Sapiński, B.; Kozieł, A. Automotive MR Shock Absorber Behaviour Considering Temperature Changes: Experimental Testing and Analysis. *Acta Mech. Autom.* **2020**, *14*, 28–34. [CrossRef]
15. Büyükköprü, M.; Uzunsoy, E.; Satar, Z.; Küçük, Y. Hysteresis Modeling of Automotive Electrohydraulic Semi-Active Dampers Using Tangent Functions and Simulation-Based Ride Comfort Evaluation. *Eng. Proc.* **2026**, *121*, 24. [CrossRef]
16. Słomczyński, M.; Radkowski, S.; Makowski, M. Model of a Quarter Car Suspension with a Damper Containing Magnetorheological Fluid and with Damaged Parts Controlled by Backstepping Method. *Energies* **2023**, *16*, 3044. [CrossRef]
17. Tabacu, C. Contributions to the Experimentation, Modeling and Simulation of a Magnetorheological Damper. Ph.D. Thesis, University of Pitești, Pitești, Romania, 2009. (In Romanian)
18. Lv, H.; Sun, Q.; Zhang, W.J. A Comparative Study of Four Parametric Hysteresis Models for Magnetorheological Dampers. *Actuators* **2021**, *10*, 257. [CrossRef]
19. Zheng, H.; Wang, X.; Li, Y. Theoretical Analysis of IGAO-Fuzzy PID Fault-Tolerant Control and Performance Optimization for Electro-Hydraulic Active Suspensions Under Internal Leakage Faults. *Actuators* **2026**, *15*, 149. [CrossRef]
20. An-Nizhami, A.; Sriyanto, N.B.; Sumiyarso, B.; Ulum, S.N.; Riadini, E.R.; Widodo, I.G. Experimental and Numerical Study of Shock Absorber Characterization and the Implication on the Dynamics of Half Vehicle Suspension System Model. *J. Rekayasa Mesin* **2023**, *18*, 409–418. [CrossRef]
21. Gardulski, J. Testing Methods for Vehicle Shock Absorbers. *J. KONES Powertrain Transp.* **2008**, *15*, 77–88.

22. Drobiszewski, J.; Łozia, Z.; Zdanowicz, P. Simulation and Experimental Assessment of the Usability of the Phase Angle Method of Examining the State of Shock Absorbers Installed in a Vehicle. *Appl. Sci.* **2024**, *14*, 10804. [CrossRef]
23. Worden, K.; Hickey, D.; Haroon, M.; Adams, D.E. Nonlinear System Identification of Automotive Dampers: A Time- and Frequency-Domain Analysis. *Mech. Syst. Signal Process.* **2009**, *23*, 104–126. [CrossRef]
24. Pazooki, A.; Goodarzi, A.; Khajepour, A.; Soltani, A. A Novel Approach for the Design and Analysis of Nonlinear Dampers for Automotive Suspensions. *J. Vib. Control.* **2017**, *24*, 3132–3147. [CrossRef]
25. Li, W.; Zhao, J.; Liu, M. Research on Current Drive System of Magnetorheological Damper Based on Fuzzy PI Control. *Materials* **2022**, *15*, 8893. [CrossRef] [PubMed]
26. Marcu, S. Research on Active Suspensions—Case Study: Passenger Cars. Ph.D. Thesis, University of Craiova, Craiova, Romania, 2023. (In Romanian)
27. Sadeghian, M.; Pilkauskas, K.; Palevičius, P.; Ragulskienė, J.; Janušas, G.; Dorešvas, V.; Palevičius, A. A Nonlinear Damper with Dynamic Load and an Elastic Slit Membrane: Modeling and Interaction Analysis. *Micromachines* **2024**, *15*, 1320. [CrossRef] [PubMed]